Supplementary Information

Dynamical Calculations of O(^3P) + OH($^2\Pi$) reaction on the CHIPR Potential Energy Surface using Fully Coupled Time-Dependent Wave-Packet Approach in Hyperspherical Coordinates

Sandip Ghosh,[1] Rahul Sharma,[2] Satrajit Adhikari[1*] and António J. C. Varandas[3,4,5†]

[1] *School of Chemical Sciences,*

Indian Association for the Cultivation of Science, Kolkata -700 032, India

[2] *Department of Chemistry, St. Xaviers' College, Kolkata-700016, West Bengal, India*

[3] *School of Physics and Physical Engineering, Qufu Normal University, 273165 Qufu, China*

[4] *Department of Physics, Universidade Federal do Espírito Santo, 29075-910 Victória, Brazil*

[5] *Departamento de Química, and Centro de Química, Universidade de Coimbra*

3004-535 Coimbra, Portugal

[*] Corresponding author. e-mail: pcsa@iacs.res.in

[†] Corresponding author. e-mail: varandas@uc.pt

S1 Channel dependence of scattering amplitudes

While calculating the scattering amplitudes, various channels (i) are distinguished by using the channel dependent amplitudes as follows:

$$\begin{aligned} u^{J,i}_{v'j'l'}(R;t) &= 4R\int dr_i \int d\eta_i\, r_i \sin\eta_i\, \rho_i^{-5/2}(\sin 2\theta)^{-1/2}\phi_{v'j'}(r_i) \\ &\times \sum_{K\mu'} g_{j'l'\mu'} A^*_{K\mu'} C_{j'\mu'}(\eta_i)\Phi^a_K(\rho_i,\theta,\phi), \end{aligned} \tag{S1}$$

with Clebsch-Gordon coefficient being

$$g_{jl\mu} = \sqrt{2\pi(2l+1)}(-1)^{j-l}\begin{pmatrix} j & l & J \\ \mu & 0 & -\mu \end{pmatrix}.$$

The integration is performed over the (θ, ϕ) grid using the transformation from Jacobi (R, r_i, η_i) to hyperspherical (ρ_i, θ, ϕ) coordinates:

$$\begin{aligned} \rho_i &= \sqrt{2}d_i\, R/\sqrt{1-\sin\theta\cos(\phi-\varepsilon_i)}\,, \\ r_i &= \frac{d_i\,\rho_i}{\sqrt{2}}\sqrt{1+\sin\theta\cos(\phi-\varepsilon_i)}\,, \\ \sin\eta_i &= \cos\theta/\sqrt{1-\sin^2\theta\cos^2(\phi-\varepsilon_i)}\,, \end{aligned}$$

with the Jacobi factor (for fixed R) given by:

$$J_i(r,\eta|\theta,\phi) = \frac{d_i^2 R\sin\theta}{[1-\sin\theta\cos(\phi-\varepsilon_i)]\sqrt{1-\sin^2\theta\cos^2(\phi-\varepsilon_i)}}, \tag{S2}$$

where the channel dependent constants, d_i and ε_i can be represented in terms of Johnson's hyperspherical coordinates as:[1,2]

$$\begin{aligned} d_i^2 &= \frac{m_i}{\mu}\left(1-\frac{m_i}{M}\right), \\ M &= \sum_i m_i\,, \\ \mu^2 &= \frac{\prod_i m_i}{M}\,, \end{aligned} \tag{S3}$$

and

$$\begin{aligned} \varepsilon_1 &= \tan^{-1}\frac{m_3}{\mu}\,, \\ \varepsilon_2 &= 0.0\,, \\ \varepsilon_3 &= -\tan^{-1}\frac{m_2}{\mu}\,. \end{aligned} \tag{S4}$$

with m_2 and m_3 being the mass of each oxygen atom.

It is noteworthy that total number of channels are not dependent on the initial rotational states (j = 0 or 1). However, the channel dependent scattering amplitudes depend on the final rotational (j'), vibrational (v') and orbital angular momentum (l') states as well as different K-component waves, where K takes the value from $+J$ to $-J$.

Grid Size	
N_ρ	256
N_θ	64
N_ϕ	128
(ρ_{min}, ρ_{max})/Å	(1.0, 15.0)
Translational Wave Packet:	
R_0/Å	4.50 ($\sim$ 4.65)†
σ/Å	0.21
k_0 (Å^{-1})	34.3991
Initial State:	
$E_{vj=0,1}$ (eV)	0.2289; 0.2334
Propagation:	
Δ t (10^{-16} s)	0.50
Magnitude of the five last Lanczos vectors*	$10^{-8} - 10^{-7}$
Absorbing Potential:	
V_{opt}/eV	0.163
ρ_I (Å)	10.5
Range of the absorbing potential (Å)	10.5 - 15.0
Projection:	
R* (Å)	4.25 ($\sim$ 5.20)†
vib. states	$v' = 0, \cdots, 5$
rot. states	$j' = 0, \cdots, 10$

Table S1: Data for initialization, projection, and absorbing potential discussed in the text: $v = 0, j = 0, 1$; $J = 0 - 50$. [† The transformed values of various parameters in ρ - space are shown in the parenthesis.]

* All vectors are normalized.

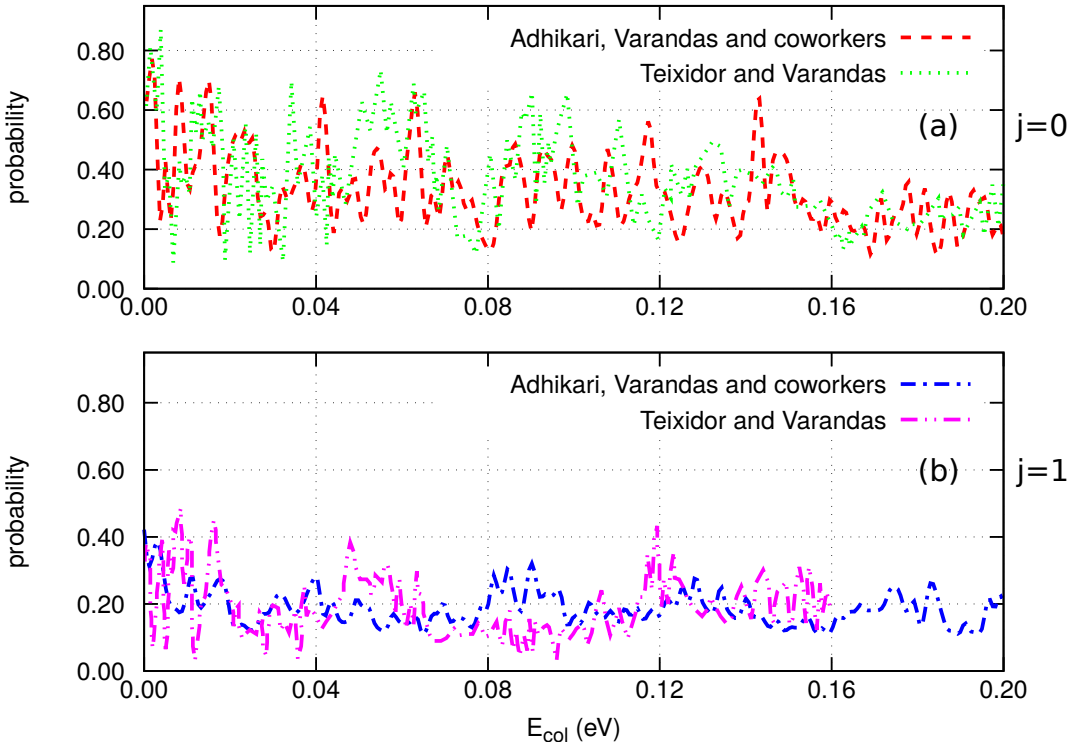

Figure S1: Total reaction probabilities for O + OH (v=0, j=0 and 1)[3] reaction performed on the CHIPR PES as a function of collision energy for J=0 case in comparison to that calculated by Teixidor and Varandas.[4]

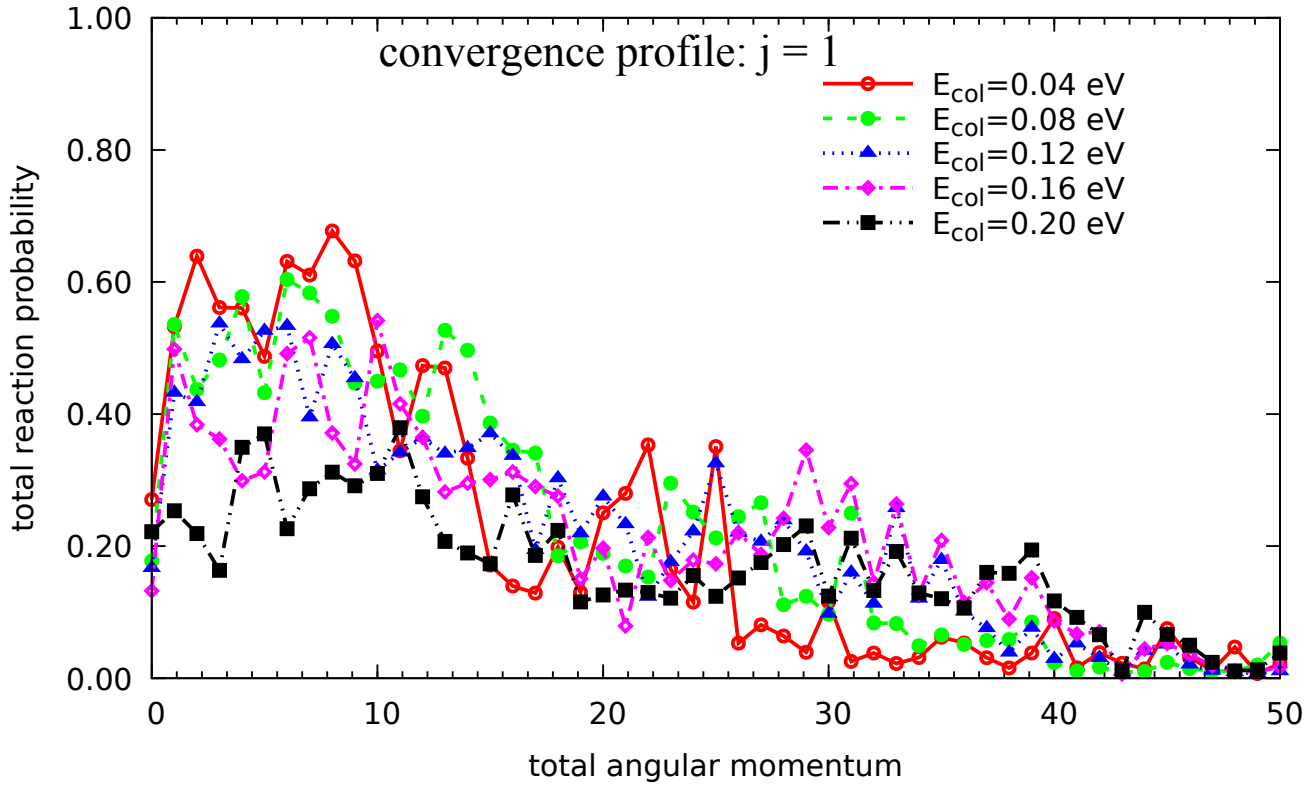

Figure S2: Convergence of total reaction probabilities with respect to total angular momentum for O + OH (v=0, j=1) reaction at five different collision energies.

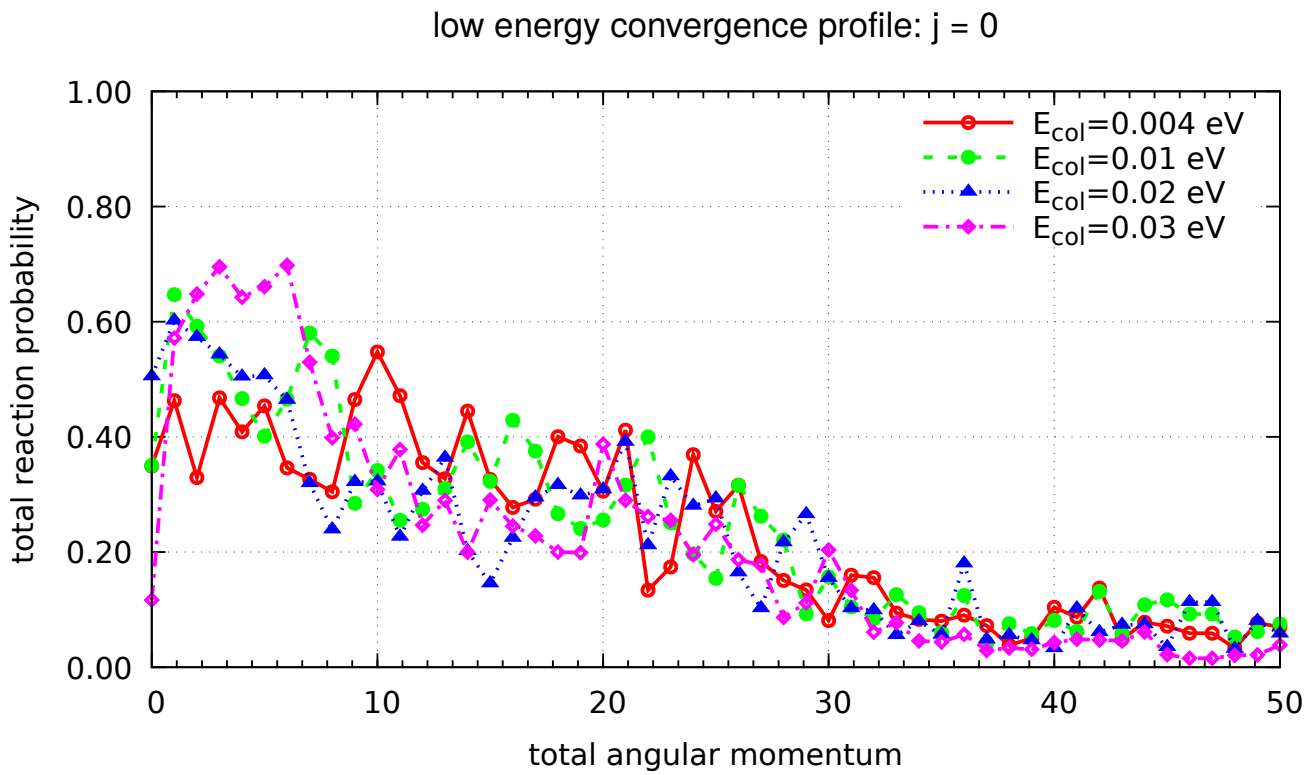

Figure S3: Convergence of total reaction probabilities with respect to total angular momentum for O + OH (v=0, j=0) reaction at very low collision energies ($\sim 10^{-3}$ eV $< E_{col} <$ 0.04 eV).

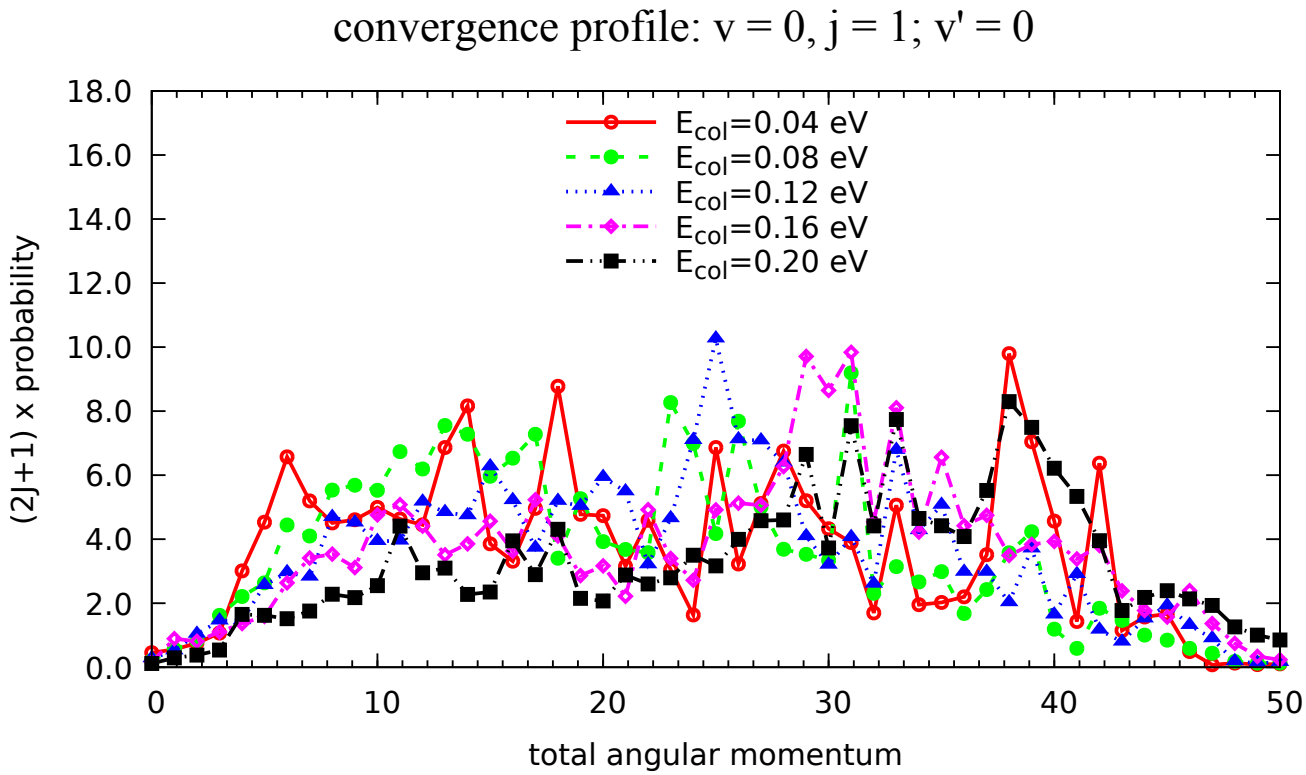

Figure S4: (2J+1)-weighted vibrationally resolved reaction probabilities as a function of total angular momentum for O+OH (v=0, j=1) $\rightarrow$ H+O_2 ($v' = 0$) reaction process at different collision energies.

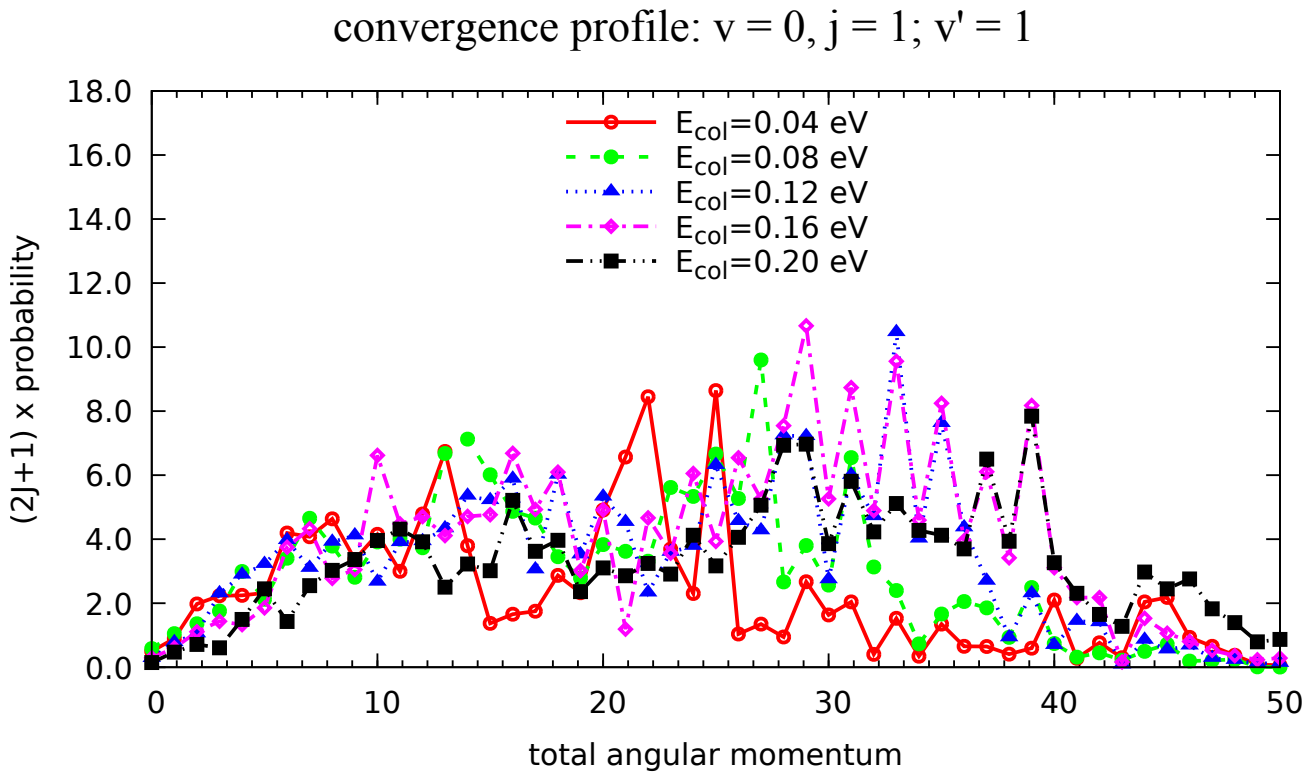

Figure S5: (2J+1)-weighted vibrationally resolved reaction probabilities as a function of total angular momentum for O+OH (v=0, j=1) $\rightarrow$ H+O_2 ($v' = 1$) reaction process at different collision energies.

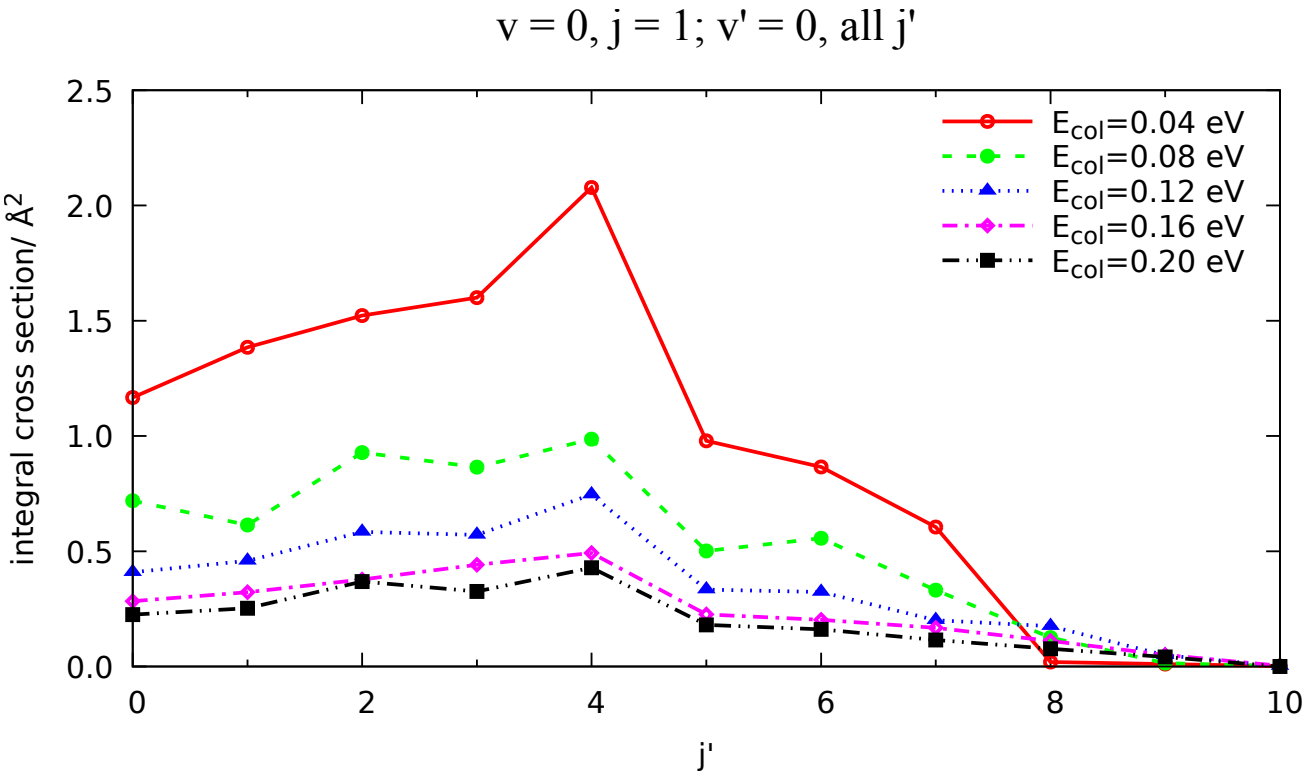

Figure S6: Rotationally resolved integral cross sections for O + OH (v=0, j=1) $\rightarrow$ H + O_2 ($v' = 0, j'$) reaction process at E_{col} = 0.04, 0.08, 0.12, 0.16 and 0.20 eV.

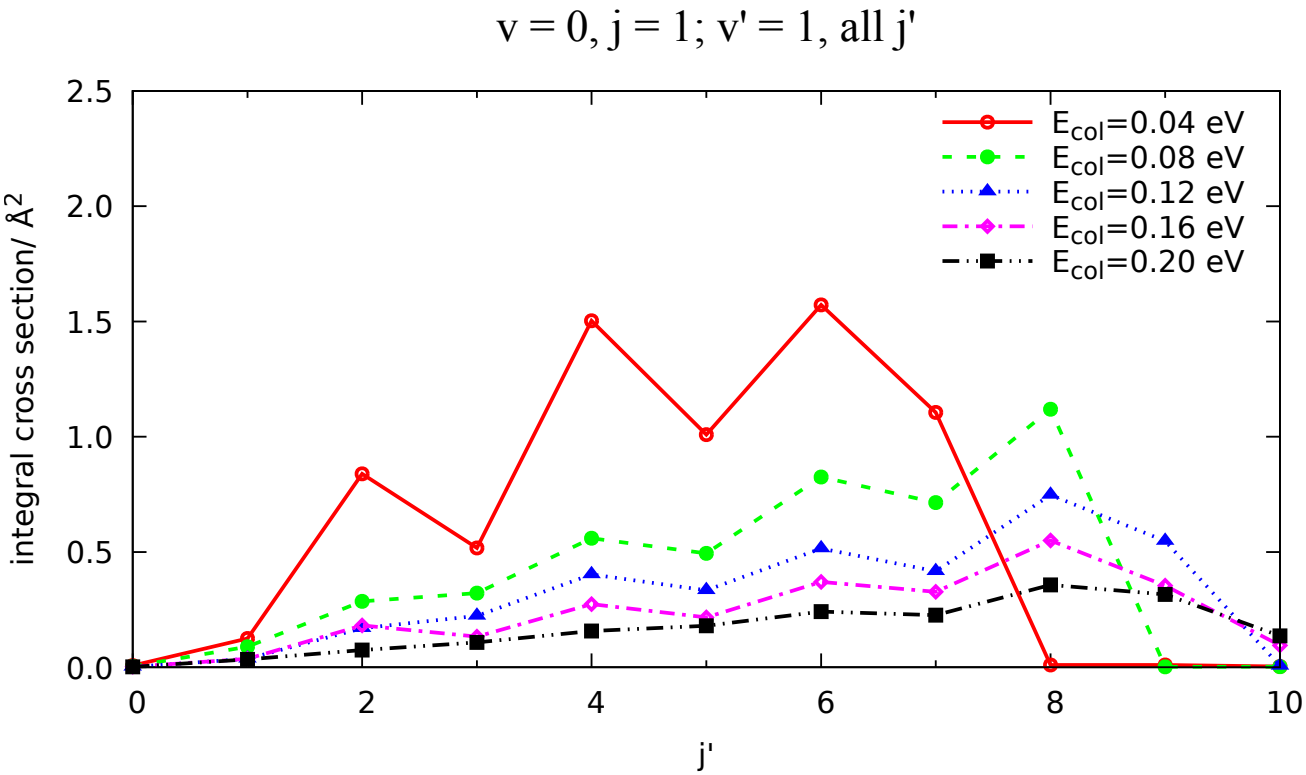

Figure S7: Rotationally resolved integral cross sections for O + OH (v=0, j=1) $\rightarrow$ H + O_2 ($v' = 1, j'$) reaction process at E_{col} = 0.04, 0.08, 0.12, 0.16 and 0.20 eV.

Figure S8, S9 and S10 describe the change of centrifugal energy, $E^{\theta}_{cent} = \frac{\hbar^2 J(J+1)}{2\mu\rho^2\cos^2\theta}$ (see fourth term of Eq. 4 in main text) as a function of J at θ = 10°, 45° and 80°, respectively for various ρ values. It may be noted that we perform the projection of outgoing wavepacket at quite large value of hyperradius around $\rho = 5.20\,\AA$, where the change of E_{cent} is quite small with the increase of J as compared to smaller ρ values. Moreover, due to the heavy mass of O atoms, the change in centrifugal barrier is further smaller and as a consequence, the Js required for convergence do not increase sharply. On the other hand, at collision energy of ∼0.04 eV, it is noticeable that the centrifugal barrier created in the asymptotic range of higher ρ values up to $J \sim 35$ case could be overcome [see Table S2], whereas for further higher Js, the barrier becomes higher to be overcome. As a result, at such low collision energy, reaction probabilities decreases with the increase of J. On the contrary, as the collision energy increases beyond 0.04 eV, the energy required to surmount the centrifugal barrier is much less for higher Js. Therefore, reaction probabilities tend to increase for higher Js with the increment of collision energy.

J	E^{10}_{cent} (eV)		E^{45}_{cent} (eV)		E^{80}_{cent} (eV)	
15	0.0068		0.0133		0.2201	
		$\Delta E^{10}_{cent} = 0.0197$		$\Delta E^{45}_{cent} = 0.0382$		$\Delta E^{80}_{cent} = 0.6327$
30	0.0265		0.0514		0.8527	
		$\Delta E^{10}_{cent} = 0.0324$		$\Delta E^{45}_{cent} = 0.0630$		$\Delta E^{80}_{cent} = 1.0453$
45	0.0590		0.1145		1.8980	

Table S2: Change of centrifugal energy for different J values at ρ = 5.20 $\AA$.

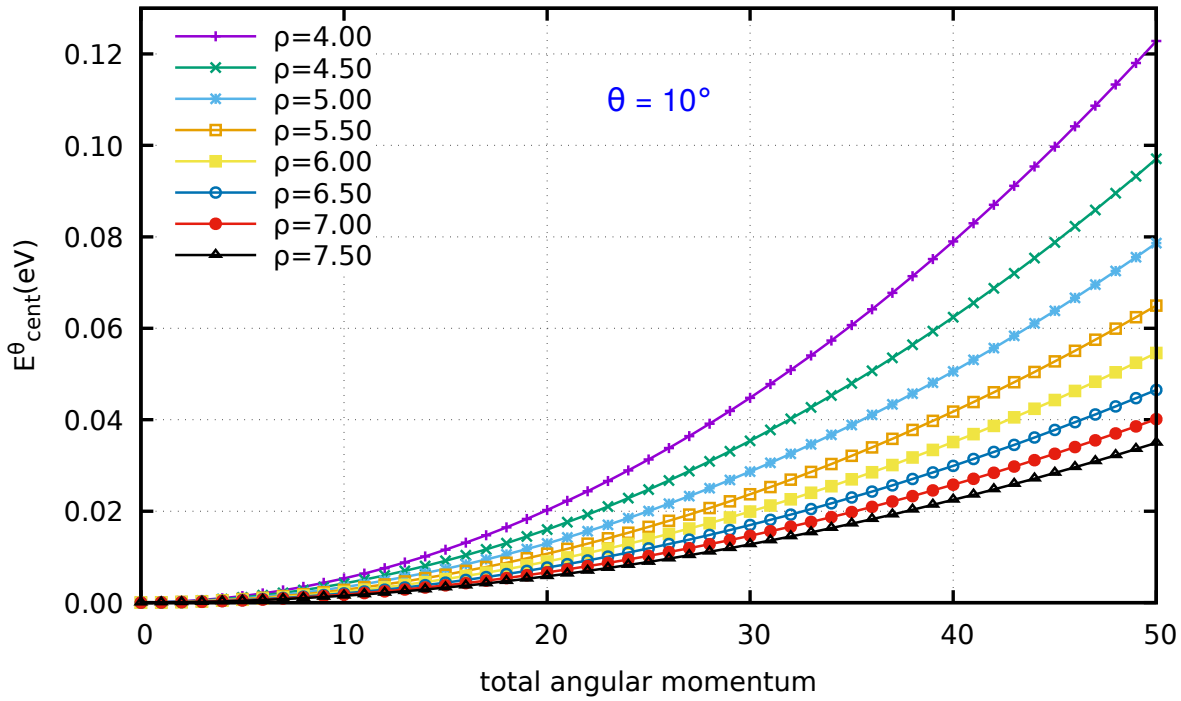

Figure S8: Centrifugal energy as a function of total angular momentum (J) at different values of the hyperradius (ρ) at $\theta = 10°$.

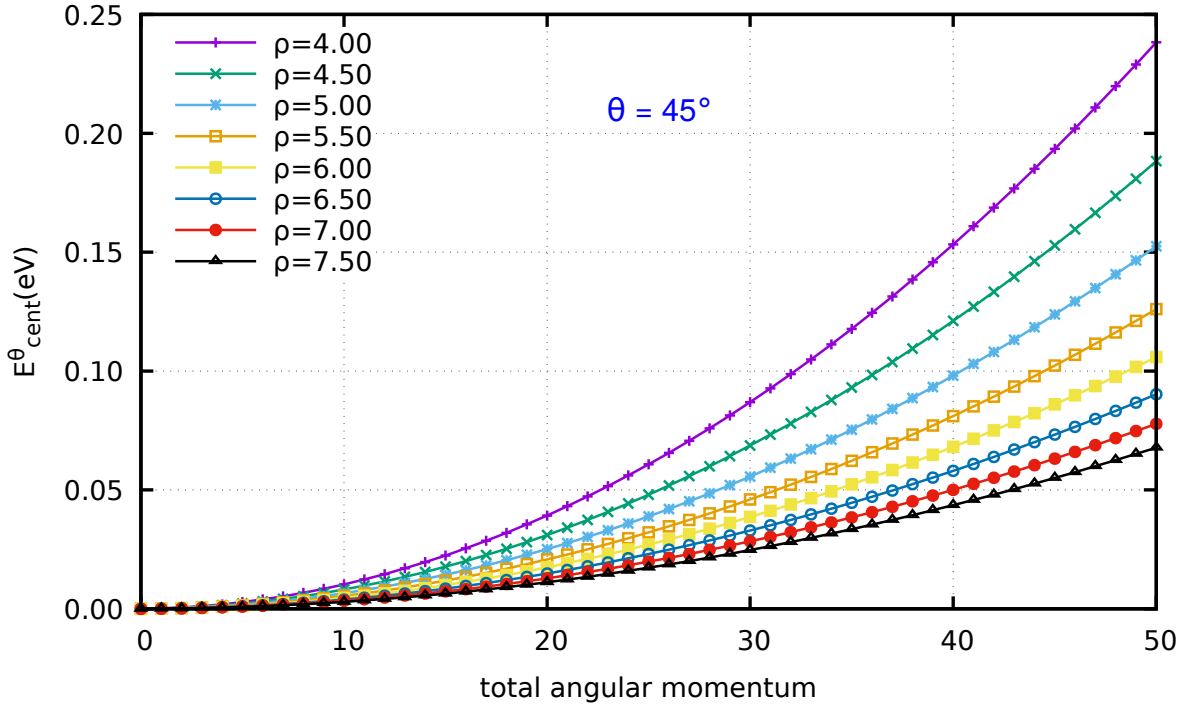

Figure S9: Same as Figure S8, but for $\theta = 45°$.

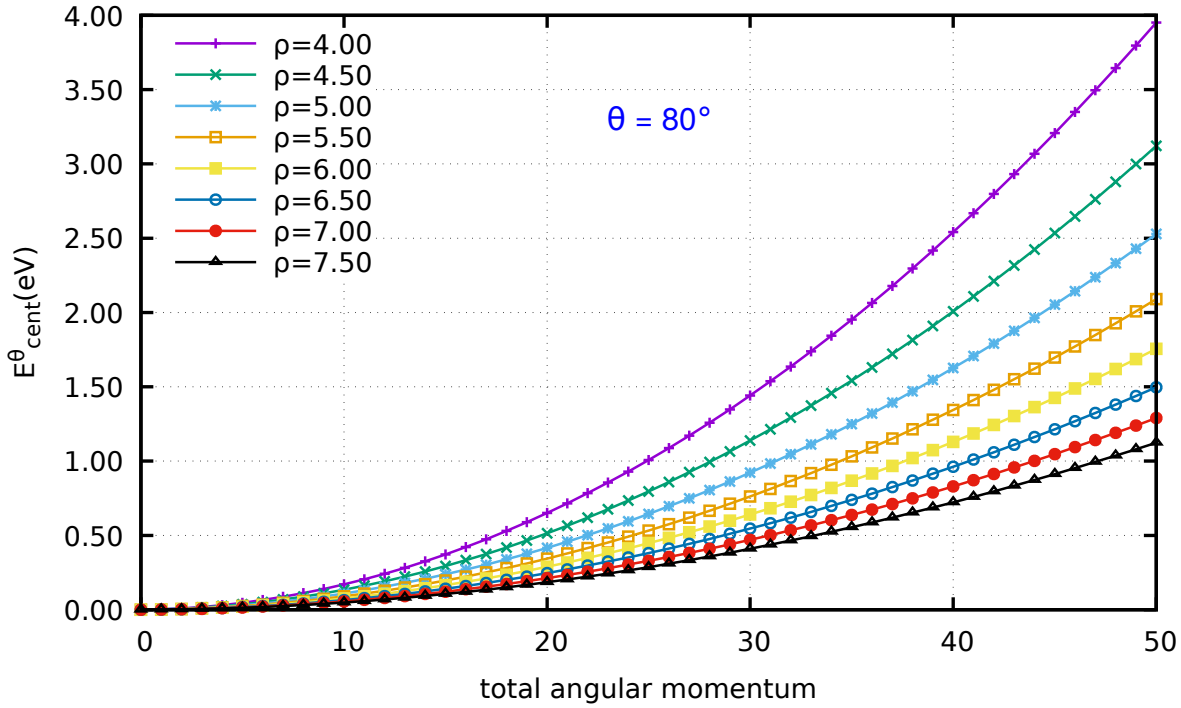

Figure S10: Same as Figure S8, but for $\theta = 80°$.

References

[1] B. R. Johnson, *J. Chem. Phys.*, 1980, **73**, 5051–5058.

[2] B. R. Johnson, *J. Chem. Phys.*, 1983, **79**, 1916–1925.

[3] S. Ghosh, R. Sharma, S. Adhikari and A. J. C. Varandas, *Chem. Phys. Lett.*, 2017, **675**, 85–91.

[4] M. M. Teixidor and A. J. C. Varandas, *J. Chem. Phys.*, 2015, **142**, 014309/1–10.